Search for $Z_c(3900)^{\pm} \to \omega\pi^{\pm}$

M. Ablikim,[1] M. N. Achasov,[9,f] X. C. Ai,[1] O. Albayrak,[5] M. Albrecht,[4] D. J. Ambrose,[44] A. Amoroso,[48a,48c] F. F. An,[1] Q. An,[45,a] J. Z. Bai,[1] R. Baldini Ferroli,[20a] Y. Ban,[31] D. W. Bennett,[19] J. V. Bennett,[5] M. Bertani,[20a] D. Bettoni,[21a] J. M. Bian,[43] F. Bianchi,[48a,48c] E. Boger,[23,d] I. Boyko,[23] R. A. Briere,[5] H. Cai,[50] X. Cai,[1,a] O. Cakir,[40a,b] A. Calcaterra,[20a] G. F. Cao,[1] S. A. Cetin,[40b] J. F. Chang,[1,a] G. Chelkov,[23,d,e] G. Chen,[1] H. S. Chen,[1] H. Y. Chen,[2] J. C. Chen,[1] M. L. Chen,[1,a] S. J. Chen,[29] X. Chen,[1,a] X. R. Chen,[26] Y. B. Chen,[1,a] H. P. Cheng,[17] X. K. Chu,[31] G. Cibinetto,[21a] H. L. Dai,[1,a] J. P. Dai,[34] A. Dbeyssi,[14] D. Dedovich,[23] Z. Y. Deng,[1] A. Denig,[22] I. Denysenko,[23] M. Destefanis,[48a,48c] F. De Mori,[48a,48c] Y. Ding,[27] C. Dong,[30] J. Dong,[1,a] L. Y. Dong,[1] M. Y. Dong,[1,a] S. X. Du,[52] P. F. Duan,[1] E. E. Eren,[40b] J. Z. Fan,[39] J. Fang,[1,a] S. S. Fang,[1] X. Fang,[45,a] Y. Fang,[1] L. Fava,[48b,48c] F. Feldbauer,[22] G. Felici,[20a] C. Q. Feng,[45,a] E. Fioravanti,[21a] M. Fritsch,[14,22] C. D. Fu,[1] Q. Gao,[1] X. Y. Gao,[2] Y. Gao,[39] Z. Gao,[45,a] I. Garzia,[21a] C. Geng,[45,a] K. Goetzen,[10] W. X. Gong,[1,a] W. Gradl,[22] M. Greco,[48a,48c] M. H. Gu,[1,a] Y. T. Gu,[12] Y. H. Guan,[1] A. Q. Guo,[1] L. B. Guo,[28] Y. Guo,[1] Y. P. Guo,[22] Z. Haddadi,[25] A. Hafner,[22] S. Han,[50] Y. L. Han,[1] X. Q. Hao,[15] F. A. Harris,[42] K. L. He,[1] Z. Y. He,[30] T. Held,[4] Y. K. Heng,[1,a] Z. L. Hou,[1] C. Hu,[28] H. M. Hu,[1] J. F. Hu,[48a,48c] T. Hu,[1,a] Y. Hu,[1] G. M. Huang,[6] G. S. Huang,[45,a] H. P. Huang,[50] J. S. Huang,[15] X. T. Huang,[33] Y. Huang,[29] T. Hussain,[47] Q. Ji,[1] Q. P. Ji,[30] X. B. Ji,[1] X. L. Ji,[1,a] L. L. Jiang,[1] L. W. Jiang,[50] X. S. Jiang,[1,a] X. Y. Jiang,[30] J. B. Jiao,[33] Z. Jiao,[17] D. P. Jin,[1,a] S. Jin,[1] T. Johansson,[49] A. Julin,[43] N. Kalantar-Nayestanaki,[25] X. L. Kang,[1] X. S. Kang,[30] M. Kavatsyuk,[25] B. C. Ke,[5] P. Kiese,[22] R. Kliemt,[14] B. Kloss,[22] O. B. Kolcu,[40b,i] B. Kopf,[4] M. Kornicer,[42] W. Kühn,[24] A. Kupsc,[49] J. S. Lange,[24] M. Lara,[19] P. Larin,[14] C. Leng,[48c] C. Li,[49] C. H. Li,[1] Cheng Li,[45,a] D. M. Li,[52] F. Li,[1,a] G. Li,[1] H. B. Li,[1] J. C. Li,[1] Jin Li,[32] K. Li,[13] K. Li,[33] Lei Li,[3] P. R. Li,[41] T. Li,[33] W. D. Li,[1] W. G. Li,[1] X. L. Li,[33] X. M. Li,[12] X. N. Li,[1,a] X. Q. Li,[30] Z. B. Li,[38] H. Liang,[45,a] Y. F. Liang,[36] Y. T. Liang,[24] G. R. Liao,[11] D. X. Lin,[14] B. J. Liu,[1] C. X. Liu,[1] F. H. Liu,[35] Fang Liu,[1] Feng Liu,[6] H. B. Liu,[12] H. H. Liu,[16] H. H. Liu,[1] H. M. Liu,[1] J. Liu,[1] J. B. Liu,[45,a] J. P. Liu,[50] J. Y. Liu,[1] K. Liu,[39] K. Y. Liu,[27] L. D. Liu,[31] P. L. Liu,[1,a] Q. Liu,[41] S. B. Liu,[45,a] X. Liu,[26] X. X. Liu,[41] Y. B. Liu,[30] Z. A. Liu,[1,a] Zhiqiang Liu,[1] Zhiqing Liu,[22] H. Loehner,[25] X. C. Lou,[1,a,h] H. J. Lu,[17] J. G. Lu,[1,a] R. Q. Lu,[18] Y. Lu,[1] Y. P. Lu,[1,a] C. L. Luo,[28] M. X. Luo,[51] T. Luo,[42] X. L. Luo,[1,a] M. Lv,[1] X. R. Lyu,[41] F. C. Ma,[27] H. L. Ma,[1] L. L. Ma,[33] Q. M. Ma,[1] T. Ma,[1] X. N. Ma,[30] X. Y. Ma,[1,a] F. E. Maas,[14] M. Maggiora,[48a,48c] Y. J. Mao,[31] Z. P. Mao,[1] S. Marcello,[48a,48c] J. G. Messchendorp,[25] J. Min,[1,a] T. J. Min,[1] R. E. Mitchell,[19] X. H. Mo,[1,a] Y. J. Mo,[6] C. Morales Morales,[14] K. Moriya,[19] N. Yu. Muchnoi,[9,f] H. Muramatsu,[43] Y. Nefedov,[23] F. Nerling,[14] I. B. Nikolaev,[9,f] Z. Ning,[1,a] S. Nisar,[8] S. L. Niu,[1,a] X. Y. Niu,[1] S. L. Olsen,[32] Q. Ouyang,[1,a] S. Pacetti,[20b] P. Patteri,[20a] M. Pelizaeus,[4] H. P. Peng,[45,a] K. Peters,[10] J. Pettersson,[49] J. L. Ping,[28] R. G. Ping,[1] R. Poling,[43] V. Prasad,[1] Y. N. Pu,[18] M. Qi,[29] S. Qian,[1,a] C. F. Qiao,[41] L. Q. Qin,[33] N. Qin,[50] X. S. Qin,[1] Y. Qin,[31] Z. H. Qin,[1,a] J. F. Qiu,[1] K. H. Rashid,[47] C. F. Redmer,[22] H. L. Ren,[18] M. Ripka,[22] G. Rong,[1] Ch. Rosner,[14] X. D. Ruan,[12] V. Santoro,[21a] A. Sarantsev,[23,g] M. Savrié,[21b] K. Schoenning,[49] S. Schumann,[22] W. Shan,[31] M. Shao,[45,a] C. P. Shen,[2] P. X. Shen,[30] X. Y. Shen,[1] H. Y. Sheng,[1] W. M. Song,[1] X. Y. Song,[1] S. Sosio,[48a,48c] S. Spataro,[48a,48c] G. X. Sun,[1] J. F. Sun,[15] S. S. Sun,[1] Y. J. Sun,[45,a] Y. Z. Sun,[1] Z. J. Sun,[1,a] Z. T. Sun,[19] C. J. Tang,[36] X. Tang,[1] I. Tapan,[40c] E. H. Thorndike,[44] M. Tiemens,[25] M. Ullrich,[24] I. Uman,[40b] G. S. Varner,[42] B. Wang,[30] B. L. Wang,[41] D. Wang,[31] D. Y. Wang,[31] K. Wang,[1,a] L. L. Wang,[1] L. S. Wang,[1] M. Wang,[33] P. Wang,[1] P. L. Wang,[1] S. G. Wang,[31] W. Wang,[1,a] X. F. Wang,[39] Y. D. Wang,[14] Y. F. Wang,[1,a] Y. Q. Wang,[22] Z. Wang,[1,a] Z. G. Wang,[1,a] Z. H. Wang,[45,a] Z. Y. Wang,[1] T. Weber,[22] D. H. Wei,[11] J. B. Wei,[31] P. Weidenkaff,[22] S. P. Wen,[1] U. Wiedner,[4] M. Wolke,[49] L. H. Wu,[1] Z. Wu,[1,a] L. G. Xia,[39] Y. Xia,[18] D. Xiao,[1] Z. J. Xiao,[28] Y. G. Xie,[1,a] Q. L. Xiu,[1,a] G. F. Xu,[1] L. Xu,[1] Q. J. Xu,[13] Q. N. Xu,[41] X. P. Xu,[37] L. Yan,[45,a] W. B. Yan,[45,a] W. C. Yan,[45,a] Y. H. Yan,[18] H. J. Yang,[34] H. X. Yang,[1] L. Yang,[50] Y. Yang,[6] Y. X. Yang,[11] H. Ye,[1] M. Ye,[1,a] M. H. Ye,[7] J. H. Yin,[1] B. X. Yu,[1,a] C. X. Yu,[30] H. W. Yu,[31] J. S. Yu,[26] C. Z. Yuan,[1] W. L. Yuan,[29] Y. Yuan,[1] A. Yuncu,[40b,c] A. A. Zafar,[47] A. Zallo,[20a] Y. Zeng,[18] B. X. Zhang,[1] B. Y. Zhang,[1,a] C. Zhang,[29] C. C. Zhang,[1] D. H. Zhang,[1] H. H. Zhang,[38] H. Y. Zhang,[1,a] J. J. Zhang,[1] J. L. Zhang,[1] J. Q. Zhang,[1] J. W. Zhang,[1,a] J. Y. Zhang,[1] J. Z. Zhang,[1] K. Zhang,[1] L. Zhang,[1] S. H. Zhang,[1] X. Y. Zhang,[33] Y. Zhang,[1] Y. N. Zhang,[41] Y. H. Zhang,[1,a] Y. T. Zhang,[45,a] Yu Zhang,[41] Z. H. Zhang,[6] Z. P. Zhang,[45] Z. Y. Zhang,[50] G. Zhao,[1] J. W. Zhao,[1,a] J. Y. Zhao,[1] J. Z. Zhao,[1,a] Lei Zhao,[45,a] Ling Zhao,[1] M. G. Zhao,[30] Q. Zhao,[1] Q. W. Zhao,[1] S. J. Zhao,[52] T. C. Zhao,[1] Y. B. Zhao,[1,a] Z. G. Zhao,[45,a] A. Zhemchugov,[23,d] B. Zheng,[46] J. P. Zheng,[1,a] W. J. Zheng,[33] Y. H. Zheng,[41] B. Zhong,[28] L. Zhou,[1,a] Li Zhou,[30] X. Zhou,[50] X. K. Zhou,[45,a] X. R. Zhou,[45,a] X. Y. Zhou,[1] K. Zhu,[1] K. J. Zhu,[1,a] S. Zhu,[1] X. L. Zhu,[39] Y. C. Zhu,[45,a] Y. S. Zhu,[1] Z. A. Zhu,[1] J. Zhuang,[1,a] L. Zotti,[48a,48c] B. S. Zou,[1] and J. H. Zou[1]

(BESIII Collaboration)

[1]*Institute of High Energy Physics, Beijing 100049, People's Republic of China*
[2]*Beihang University, Beijing 100191, People's Republic of China*
[3]*Beijing Institute of Petrochemical Technology, Beijing 102617, People's Republic of China*
[4]*Bochum Ruhr-University, D-44780 Bochum, Germany*
[5]*Carnegie Mellon University, Pittsburgh, Pennsylvania 15213, USA*
[6]*Central China Normal University, Wuhan 430079, People's Republic of China*

[7]*China Center of Advanced Science and Technology, Beijing 100190, People's Republic of China*
[8]*COMSATS Institute of Information Technology, Lahore, Defence Road, Off Raiwind Road, 54000 Lahore, Pakistan*
[9]*G.I. Budker Institute of Nuclear Physics SB RAS (BINP), Novosibirsk 630090, Russia*
[10]*GSI Helmholtzcentre for Heavy Ion Research GmbH, D-64291 Darmstadt, Germany*
[11]*Guangxi Normal University, Guilin 541004, People's Republic of China*
[12]*GuangXi University, Nanning 530004, People's Republic of China*
[13]*Hangzhou Normal University, Hangzhou 310036, People's Republic of China*
[14]*Helmholtz Institute Mainz, Johann-Joachim-Becher-Weg 45, D-55099 Mainz, Germany*
[15]*Henan Normal University, Xinxiang 453007, People's Republic of China*
[16]*Henan University of Science and Technology, Luoyang 471003, People's Republic of China*
[17]*Huangshan College, Huangshan 245000, People's Republic of China*
[18]*Hunan University, Changsha 410082, People's Republic of China*
[19]*Indiana University, Bloomington, Indiana 47405, USA*
[20a]*INFN Laboratori Nazionali di Frascati, I-00044 Frascati, Italy*
[20b]*INFN and University of Perugia, I-06100 Perugia, Italy*
[21a]*INFN Sezione di Ferrara, I-44122 Ferrara, Italy*
[21b]*University of Ferrara, I-44122 Ferrara, Italy*
[22]*Johannes Gutenberg University of Mainz, Johann-Joachim-Becher-Weg 45, D-55099 Mainz, Germany*
[23]*Joint Institute for Nuclear Research, 141980 Dubna, Moscow Region, Russia*
[24]*Justus Liebig University Giessen, II. Physikalisches Institut, Heinrich-Buff-Ring 16, D-35392 Giessen, Germany*
[25]*KVI-CART, University of Groningen, NL-9747 AA Groningen, The Netherlands*
[26]*Lanzhou University, Lanzhou 730000, People's Republic of China*
[27]*Liaoning University, Shenyang 110036, People's Republic of China*
[28]*Nanjing Normal University, Nanjing 210023, People's Republic of China*
[29]*Nanjing University, Nanjing 210093, People's Republic of China*
[30]*Nankai University, Tianjin 300071, People's Republic of China*
[31]*Peking University, Beijing 100871, People's Republic of China*
[32]*Seoul National University, Seoul 151-747, Korea*
[33]*Shandong University, Jinan 250100, People's Republic of China*
[34]*Shanghai Jiao Tong University, Shanghai 200240, People's Republic of China*
[35]*Shanxi University, Taiyuan 030006, People's Republic of China*
[36]*Sichuan University, Chengdu 610064, People's Republic of China*
[37]*Soochow University, Suzhou 215006, People's Republic of China*
[38]*Sun Yat-Sen University, Guangzhou 510275, People's Republic of China*
[39]*Tsinghua University, Beijing 100084, People's Republic of China*
[40a]*Istanbul Aydin University, 34295 Sefakoy, Istanbul, Turkey*
[40b]*Dogus University, 34722 Istanbul, Turkey*
[40c]*Uludag University, 16059 Bursa, Turkey*
[41]*University of Chinese Academy of Sciences, Beijing 100049, People's Republic of China*
[42]*University of Hawaii, Honolulu, Hawaii 96822, USA*
[43]*University of Minnesota, Minneapolis, Minnesota 55455, USA*
[44]*University of Rochester, Rochester, New York 14627, USA*
[45]*University of Science and Technology of China, Hefei 230026, People's Republic of China*
[46]*University of South China, Hengyang 421001, People's Republic of China*
[47]*University of the Punjab, Lahore-54590, Pakistan*
[48a]*University of Turin, I-10125, Turin, Italy*
[48b]*University of Eastern Piedmont, I-15121 Alessandria, Italy*
[48c]*INFN, I-10125 Turin, Italy*
[49]*Uppsala University, Box 516, SE-75120 Uppsala, Sweden*
[50]*Wuhan University, Wuhan 430072, People's Republic of China*
[51]*Zhejiang University, Hangzhou 310027, People's Republic of China*
[52]*Zhengzhou University, Zhengzhou 450001, People's Republic of China*

(Received 8 July 2015; published 28 August 2015)

The decay $Z_c(3900)^{\pm} \to \omega\pi^{\pm}$ is searched for using data samples collected with the BESIII detector operating at the BEPCII storage ring at center-of-mass energies $\sqrt{s} = 4.23$ and 4.26 GeV. No significant signal for the $Z_c(3900)^{\pm}$ is found, and upper limits at the 90% confidence level on the Born cross section for the process $e^+e^- \to Z_c(3900)^{\pm}\pi^{\mp} \to \omega\pi^+\pi^-$ are determined to be 0.26 and 0.18 pb at $\sqrt{s} = 4.23$ and 4.26 GeV, respectively.

DOI: 10.1103/PhysRevD.92.032009 PACS numbers: 14.40.Rt, 13.25.Jx, 13.66.Bc, 14.40.Pq

I. INTRODUCTION

Recently, in the study of $e^+e^- \to J/\psi\pi^+\pi^-$, a distinct charged structure, named the $Z_c(3900)^{\pm}$, was observed in the $J/\psi\pi^{\pm}$ spectrum by BESIII [1] and Belle [2]. Its existence was confirmed shortly thereafter with CLEO-c data [3]. The existence of the neutral partner in the decay $Z_c(3900)^0 \to J/\psi\pi^0$ has also been reported in CLEO-c data [3] and by BESIII [4]. The $Z_c(3900)$ is a good candidate for an exotic state beyond simple quark models, since it contains a $c\bar{c}$ pair and is also electrically charged. Noting that the $Z_c(3900)$ has a mass very close to the $D^*\bar{D}$ threshold (3875 MeV), BESIII analyzed the process $e^+e^- \to \pi^{\pm}(D\bar{D}^*)^{\mp}$, and a clear structure in the $(D\bar{D}^*)^{\mp}$ mass spectrum is seen, called the $Z_c(3885)$. The measured mass and width are $(3883.9 \pm 1.5 \pm 4.2)$ MeV/c^2 and $(24.8 \pm 3.3 \pm 11.0)$ MeV, respectively, and quantum numbers $J^P = 1^+$ are favored [5]. Assuming the $Z_c(3885) \to D\bar{D}^*$ and the $Z_c(3900) \to J/\psi\pi$ signals are from the same source, the ratio of partial widths $\frac{\Gamma(Z_c(3885)\to D\bar{D}^*)}{\Gamma(Z_c(3900)\to J/\psi\pi)}$ is determined to be $6.2 \pm 1.1 \pm 2.7$.

The observation of the $Z_c(3900)$ has stimulated many theoretical studies of its nature. Possible interpretations are tetraquark [6], hadro-charmonium [7], $D^*\bar{D}$ molecule [8] and threshold effects [9–11]. Lattice QCD studies provide theoretical support for the existence of $X(3872)$ [12] but not for the $Z_c(3900)$ [13–17]. However, those studies were carried out on small volumes with unphysically heavy up and down quarks. It is also worth noting that no resonant structure in $J/\psi\pi$ is observed in $\bar{B}^0 \to J/\psi\pi^+\pi^-$ by LHCb [18], in $\bar{B}^0 \to J/\psi K^-\pi^+$ by Belle [19] or in $\gamma p \to J/\psi\pi^+ n$ by COMPASS [20].

The decay properties of a state can provide useful information on its internal structure. There are three important decay modes for charmoniumlike states: (i) "fall-apart" decays to open charm mesons; (ii) cascades to hidden charm mesons; and (iii) decays to light hadrons via intermediate gluons. In addition, as shown in Refs. [9,10], an enhancement near the $D\bar{D}^*$ threshold can be produced via the rescattering of hidden or open charm final states. Decays of the $Z_c(3900)$ to light hadrons can play a unique role in distinguishing a resonance from threshold effects, because the decay mode with $c\bar{c}$ annihilation involves neither hidden nor open charm final states. However, theory estimates of annihilation widths to light hadrons are only an order of magnitude due to uncertainties of wave function effects and QCD corrections [21,22]. A sizable $Z_c(3900)$ decay width to light hadrons might be expected in analogy to η_c or χ_{cJ} into hadronic final states.

Among a large number of hadronic final states that are available for a $I^G(J^P) = 1^+(1^+)$ resonance decay, $\omega\pi$ is one of the typical decay modes which are not suppressed by any known selection rule. In this paper, we report a search for $Z_c(3900)^{\pm} \to \omega\pi^{\pm}$ based on e^+e^- annihilation samples taken at center-of-mass (c.m.) energies $\sqrt{s} = 4.23$ and 4.26 GeV around the peak of $Y(4260)$. The data samples were collected with the BESIII [23] detector operating at the BEPCII storage ring. The integrated luminosity of these data samples are measured by analyzing the large-angle Bhabha scattering events with an uncertainty of 1.0% [24] and are equal to 1092 and 826 pb^{-1}, for $\sqrt{s} = 4.23$ and 4.26 GeV, respectively.

II. BESIII EXPERIMENT AND MONTE CARLO SIMULATION

The BESIII detector, described in detail in Ref. [23], has a geometrical acceptance of 93% of 4π. A small-cell helium-based main drift chamber (MDC) provides a charged particle momentum resolution of 0.5% at 1 GeV/c in a 1 T magnetic field, and supplies energy-loss (dE/dx) measurements with a resolution of 6% for minimum-ionizing pions. The electromagnetic calorimeter (EMC) measures photon energies with a resolution of 2.5% (5%) at 1.0 GeV in the barrel (end caps). Particle

[a]Also at State Key Laboratory of Particle Detection and Electronics, Beijing 100049, Hefei 230026, People's Republic of China.
[b]Also at Ankara University,06100 Tandogan, Ankara, Turkey.
[c]Also at Bogazici University, 34342 Istanbul, Turkey.
[d]Also at the Moscow Institute of Physics and Technology, Moscow 141700, Russia.
[e]Also at the Functional Electronics Laboratory, Tomsk State University, Tomsk, 634050, Russia.
[f]Also at the Novosibirsk State University, Novosibirsk 630090, Russia.
[g]Also at the NRC Kurchatov Institute, PNPI, 188300 Gatchina, Russia.
[h]Also at University of Texas at Dallas, Richardson, Texas 75083, USA.
[i]Present address: Istanbul Arel University, 34295 Istanbul, Turkey.

identification (PID) is provided by a time-of-flight (TOF) system with a time resolution of 80 ps (110 ps) for the barrel (end caps). The muon system, located in the iron flux return yoke of the magnet, provides 2 cm position resolution and detects muon tracks with momenta greater than 0.5 GeV/c.

The GEANT4-based [25] Monte Carlo (MC) simulation software package includes the geometric description of the BESIII detector and a simulation of the detector response. It is used to optimize event selection criteria, estimate backgrounds and evaluate the detection efficiency. We generate signal MC samples of $e^+e^- \to Z_c(3900)^\pm\pi^\mp \to \omega\pi^+\pi^-$ uniformly in phase space, where the ω decays to $\pi^+\pi^-\pi^0$. The decays of $\omega \to \pi^+\pi^-\pi^0$ are generated with the OMEGA_DALITZ model in EVTGEN [26,27]. Initial state radiation is simulated with KKMC [28,29], where the Born cross section of $e^+e^- \to Z_c(3900)^\pm\pi^\mp$ is assumed to follow a $Y(4260)$ Breit-Wigner (BW) line shape with resonance parameters taken from the Particle Data Group (PDG) [30], which are listed as $X(4260)$. Final state radiation effects associated with charged particles are handled with PHOTOS [28]. For studies of possible backgrounds, inclusive $Y(4260)$ MC samples with luminosity equivalent to the experimental data at $\sqrt{s} = 4.23$ and $\sqrt{s} = 4.26$ GeV are generated, where the main known decay channels are generated using EVTGEN [26,27] with branching fractions taken from the PDG [30]. The remaining events associated with charmonium decays are generated with LUNDCHARM [31], while continuum hadronic events are generated with PYTHIA [32]. QED processes such as Bhabha scattering, dimuon and digamma events are generated with KKMC [28,29].

III. DATA ANALYSIS AND BACKGROUND STUDY

Tracks of charged particles in BESIII are reconstructed from MDC hits. We select tracks with their point of closest approach within ± 10 cm of the interaction point in the beam direction and within 1 cm in the plane perpendicular to the beam. Information from the TOF and dE/dx measurements are combined to form PID confidence levels for the π and K hypotheses; each track is assigned to the particle type with the highest confidence level.

Photon candidates are reconstructed by clustering EMC crystal energies. The efficiency and energy resolution are improved by including energy deposits in nearby TOF counters. The minimum energy is required to be 25 MeV for barrel showers ($|\cos\theta| < 0.80$) and 50 MeV for endcap showers ($0.86 < |\cos\theta| < 0.92$). To exclude showers from charged particles, the angle between the shower and the extrapolated charged tracks at the EMC must be greater than 5°. A requirement on the EMC cluster timing with respect to the event start time is applied to suppress electronic noise and energy deposits unrelated to the event.

The π^0 candidates are formed from pairs of photons that can be kinematically fitted to the known π^0 mass. The χ^2 from this fit with one degree of freedom is required to be less than 25.

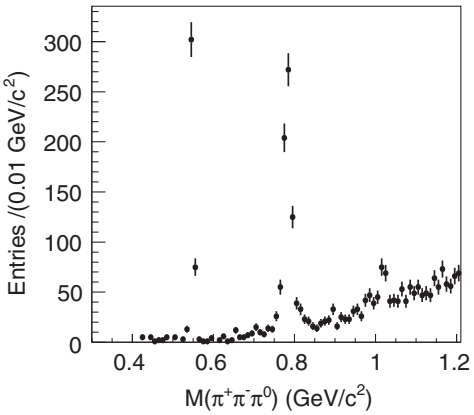

FIG. 1. The $\pi^+\pi^-\pi^0$ invariant mass distribution of the combination closest to the ω, for the selected $e^+e^- \to \pi^+\pi^-\pi^+\pi^-\pi^0$ candidates for the data sample at $\sqrt{s} = 4.23$ GeV.

Events with exactly four charged tracks identified as pions with zero net charge and at least one π^0 candidate are selected. A five-constraint kinematic fit is performed to the hypothesis of $e^+e^- \to \pi^+\pi^-\pi^+\pi^-\pi^0$ (constraints are the 4-momentum of the initial e^+e^- system and the π^0 mass), and $\chi^2_{5C} < 40$ is required. If more than one π^0 is found in an event there, the combination with the smallest χ^2_{5C} is retained.

Figure 1 shows the $\pi^+\pi^-\pi^0$ invariant mass distribution of the $\pi^+\pi^-\pi^0$ combination with invariant mass closest to the mass of ω for the selected candidate $e^+e^- \to \pi^+\pi^-\pi^+\pi^-\pi^0$ events at $\sqrt{s} = 4.23$ GeV, where prominent η, ω and ϕ signals are observed. $Z_c(3900) \to \eta\pi$ is forbidden by spin-parity conservation. We focus on the $\omega\pi^\pm$ invariant mass distribution for further study.

Candidates of ω are selected with the mass window $|M(\pi^+\pi^-\pi^0)_{\rm closest} - m_\omega| < 0.03$ GeV/c^2, where m_ω is the nominal mass of the ω taken from the PDG [30]. Figure 2

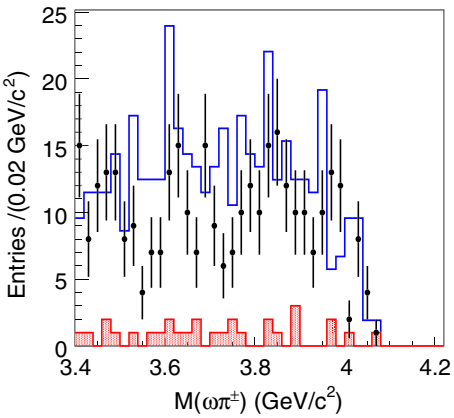

FIG. 2 (color online). Distribution of $M(\omega\pi^\pm)$ for the data sample at $\sqrt{s} = 4.23$ GeV. The dots with error bars are events within the ω signal region. The shaded histogram shows events selected from the ω sidebands, and the solid histogram shows inclusive MC events, which are dominated by continuum events.

shows the $M(\omega\pi^\pm)$ distribution for the candidate events of $e^+e^- \to \omega\pi^+\pi^-$ at $\sqrt{s} = 4.23$ GeV. No sign of a peak near 3.9 GeV/c^2 is apparent. The shaded histogram in Fig. 2 shows the distribution of the non-ω background for the events in ω sideband regions ($0.06 < |M(\pi^+\pi^-\pi^0)_{\rm closest} - m_\omega| < 0.09$ GeV/c^2).

By studying inclusive MC samples with luminosity equivalent to the data at $\sqrt{s} = 4.23$ and 4.26 GeV, the background is found to be dominantly from the continuum process $e^+e^- \to \omega\pi^+\pi^-$. The solid histogram in Fig. 2 shows the $\omega\pi^\pm$ invariant mass distribution for events selected from the inclusive MC sample.

IV. FITTING RESULTS

We use a one-dimensional, unbinned, extended maximum likelihood fit to the $\omega\pi^\pm$ invariant mass distribution to obtain the yield of $Z_c(3900)^\pm \to \omega\pi^\pm$ events. The signal probability density function is parametrized by an $\mathcal{S}$-wave Breit-Wigner function convolved with a Gaussian resolution function and weighted with the detection efficiency:

$$\left(G(M;\sigma) \otimes \frac{p\cdot q}{(M^2 - M_0^2)^2 + M_0^2\Gamma^2}\right) \times \varepsilon(M), \quad (1)$$

where $G(M;\sigma)$ is a Gaussian function representing the mass resolution. The mass resolution of the $Z_c(3900)^\pm$ is 1.2 ± 0.1 MeV/c^2 at both $\sqrt{s} = 4.23$ and 4.26 GeV, according to MC simulation. $p\cdot q$ is the S-wave phase space factor, where p is the $Z_c(3900)^\pm$ momentum in the e^+e^- c.m. frame and q is the ω momentum in the $Z_c(3900)^\pm$ c.m. frame. M is the invariant mass of $\omega\pi^\pm$, and M_0 and Γ are the mass and width of the $Z_c(3900)^\pm$, which are fixed to the results in Ref. [1]. $\varepsilon(M)$ is the efficiency curve as a function of the $\omega\pi^\pm$ invariant mass, obtained from signal MC simulation.

The background shape is described by an ARGUS function $M\sqrt{1-(M/m_0)^2}\cdot\exp(c(1-(M/m_0)^2))$, where c is left free in the fit and m_0 is fixed to the threshold of $\sqrt{s} - m_\pi$ [33].

Figure 3(a) shows the fit result for the data sample at $\sqrt{s} = 4.23$ GeV. The fit yields 14 ± 11 events for the $Z_c(3900)^\pm$ signal. Compared to the fit without the $Z_c(3900)^\pm$ signal, the change in $\ln L$ with $\Delta(\mathrm{DOF}) = 1$ is 0.74, corresponding to a statistical significance of 1.2σ. Using the Bayesian method [[30], Sec. 38.4.1], the upper limit for the $Z_c(3900)^\pm$ signal is set to 33.5 events at the 90% confidence level (C.L.), where only the statistical uncertainty is considered.

The fit result for the data sample at $\sqrt{s} = 4.26$ GeV is shown in Fig. 3(b). The fit yields 2.2 ± 8.1 events for the $Z_c(3900)^\pm$ with a statistical significance of 0.1σ. The upper limit is 18.8 events at the 90% C.L.

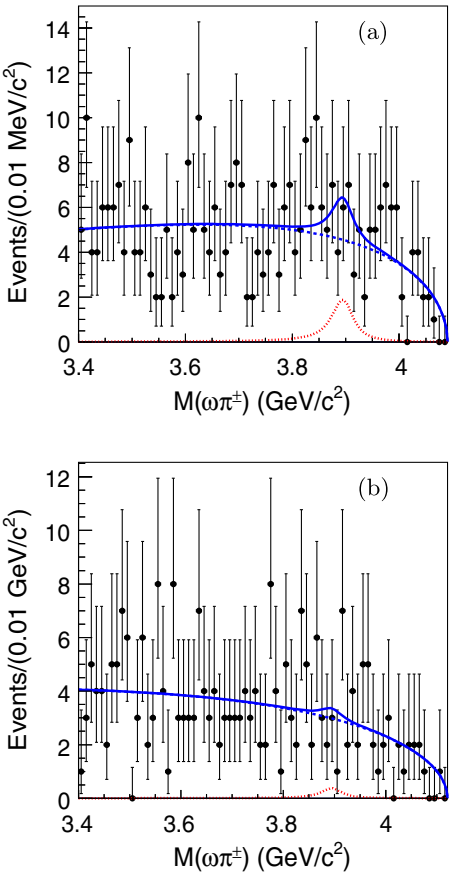

FIG. 3 (color online). Results of the unbinned maximum likelihood fit of the $\omega\pi^\pm$ mass spectrum of $e^+e^- \to \omega\pi^+\pi^-$ at (a) $\sqrt{s} = 4.23$ GeV and (b) $\sqrt{s} = 4.26$ GeV. Dots with error bars are the data. The solid curve is the result of the fit described in the text. The dotted curve is the $Z_c(3900)^\pm$ signal. The dashed curve is the background.

V. CROSS SECTION UPPER LIMITS AND SYSTEMATIC UNCERTAINTY

The upper limit on the Born cross section at the 90% C.L. is calculated as

$$\sigma(e^+e^- \to Z_c(3900)^\pm\pi^\mp, Z_c(3900)^\pm \to \omega\pi^\pm) = \frac{N^{\rm UL}}{\mathcal{L}_{\rm int}(1+\delta)\frac{1}{|1-\Pi|^2}\epsilon(1-\sigma_\epsilon)\mathcal{B}_\omega\mathcal{B}_{\pi^0}}, \quad (2)$$

where $N^{\rm UL}$ is the upper limit on the signal events; $\mathcal{L}_{\rm int}$ is the integrated luminosity; ϵ is the selection efficiency obtained from signal MC simulation, which are $18.5 \pm 0.2\%$ and $18.6 \pm 0.2\%$ at $\sqrt{s} = 4.23$ and 4.26 GeV, respectively; σ_ϵ is the systematic uncertainty of the efficiency described in the next paragraph; $\frac{1}{|1-\Pi|^2}$ is the vacuum polarization factor obtained by using calculations from Ref. [34], and equal to 1.06 for both energies; $(1+\delta)$ is the radiative correction factor, equal to 0.844 for $\sqrt{s} = 4.23$ GeV and 0.848 for $\sqrt{s} = 4.26$ GeV obtained using Refs. [28,29] by assuming

the line shape of Born cross section $\sigma(e^+e^- \to Z_c(3900)^\pm\pi^\mp)$ to be a BW function with the parameters of the $Y(4260)$ taken from PDG [30]; and $\mathcal{B}_\omega$ and $\mathcal{B}_{\pi^0}$ are the branching fractions of the decay $\omega \to \pi^+\pi^-\pi^0$ and $\pi^0 \to \gamma\gamma$ [30], respectively. A conservative estimate of the upper limit of the Born cross section is determined by lowering the efficiency by one standard deviation of the systematic uncertainty.

The systematic uncertainty of the cross section measurement from Eq. (2) is summarized in Table I. The luminosity is measured using Bhabha events with an uncertainty of 1.0% [24]. The uncertainty in tracking efficiency for pions is 1.0% per track [5], i.e. 4.0% for the track selection in this analysis. The uncertainty in PID efficiency for pions is 1.0% per track [5]. The uncertainty in the photon reconstruction efficiency is less than 1% per photon [35]. The uncertainty in the π^0 reconstruction efficiency is 2.0% [36]. The uncertainty of the kinematic fit is estimated by correcting the helix parameters of the charged tracks. The detailed procedure to extract the correction factors can be found in Ref. [37]. The track parameters in MC samples are corrected by these factors, and the difference in efficiencies of 0.8% with and without the correction is taken as the systematic uncertainty associated with the kinematic fit. A MC sample generated with $Z_c(3900)^\pm \to \omega\pi^\pm$ in both the S wave and the D wave, assuming a D/S waves amplitude ratio of 0.1, results in a 3% change in detection efficiency. This difference is taken as the systematic uncertainty associated with the MC production model. The branching ratio value for $\omega \to \pi^+\pi^-\pi^0$ comes from the PDG [30], and its error is 0.8%. In the nominal fit, the radiative correction factor and the detection efficiency are determined under the assumption that the production of $e^+e^- \to Z_c(3900)^\pm\pi^\mp$ follows the $Y(4260)$ line shape. Using the line shape of $\sigma(e^+e^- \to Z_c(3900)^0\pi^0)$ measured in Ref. [4] as an alternative assumption, $\epsilon(1+\delta)$ is increased by 6% for $\sqrt{s} = 4.23$ GeV and 7% for $\sqrt{s} = 4.26$ GeV. The change in $\epsilon(1+\delta)$ is taken as a systematic uncertainty. The uncertainty of the vacuum polarization factor is taken from Ref. [34], and is negligible compared with other uncertainties. Assuming that all sources of systematic uncertainties are independent, the total errors are given by the quadratic sums.

TABLE I. Summary of the relative systematic uncertainties of the cross section measurement (in %).

Source	$\sqrt{s} = 4.23$ GeV	$\sqrt{s} = 4.26$ GeV
Luminosity	1.0	1.0
Tracking	4.0	4.0
PID	4.0	4.0
Photon reconstruction	2.0	2.0
π^0 reconstruction	2.0	2.0
Kinematic fit	0.8	0.8
Decay model	3	3
Radiative correction	6	7
$\mathrm{Br}(\omega \to \pi^+\pi^-\pi^0)$	0.8	0.8
Total	9.4	10.1

TABLE II. Results of upper limits on the $Z_c(3900)$ signal yield with various fit procedures.

Source	$\sqrt{s} = 4.23$ GeV	$\sqrt{s} = 4.26$ GeV
Fit range	31.5	18.5
Background shape	38.0	16.1
$Z_c(3900)$ mass and width	22.6	12.2
Mass resolution	33.5	18.8
Efficiency curve	33.3	18.8

To estimate the systematic uncertainties due to the fit procedure, we fit under different scenarios, and the upper limits obtained at the 90% C.L. for the $Z_c(3900)^\pm$ signal yield are summarized in Table II. The effect on the signal yield from the fit range is obtained by varying the fit range by ± 0.1 GeV/c^2. The effect due to the choice of the background shape is estimated by changing the background shape from the ARGUS function to a second order polynomial (where the parameters of the polynomial are allowed to vary and the fit range is limited to $[3.4, 4.08]$ GeV/c^2). The effect due to the resonance parameters of the $Z_c(3900)^\pm$ is estimated by varying the resonance parameters according to the results in Ref. [5]. The effect due to the mass resolution is estimated by increasing the resolution by 10% according to the comparison between the data and MC. The effect due to the mass-dependent efficiency curve is estimated by changing the efficiency curve to a constant function. We take the largest number of $Z_c(3900)^\pm$ events in the different scenarios as a conservative estimate of the upper limit: $N^{\mathrm{UL}}_{4230} = 38.0$, $N^{\mathrm{UL}}_{4260} = 18.8$. The resulting upper limits of the Born cross sections at $\sqrt{s} = 4.23$ and 4.26 GeV are determined to be 0.26 and 0.18 pb at the 90% C.L., respectively.

VI. SUMMARY AND DISCUSSION

In summary, based on data samples of 1092 pb^{-1} at $\sqrt{s} = 4.23$ GeV and 826 pb^{-1} at $\sqrt{s} = 4.26$ GeV collected with the BESIII detector operating at the BEPCII storage ring, a search is performed for the decay $Z_c(3900)^\pm \to \omega\pi^\pm$ in $e^+e^- \to \omega\pi^+\pi^-$. No $Z_c(3900)^\pm$ signal is observed. The corresponding upper limits on the Born cross section are set to be 0.26 and 0.18 pb at $\sqrt{s} = 4.23$ and 4.26 GeV, respectively. If we assume that the $Z_c(3900)^\pm$ observed in $e^+e^- \to J/\psi\pi^+\pi^-$ [1] and $Z_c(3885)^\pm$ in $e^+e^- \to (D\bar{D}^*)^\pm\pi^\mp$ [5] are the same particle, the decay width of $Z_c(3900)^\pm \to \omega\pi^\pm$ is estimated to be smaller than 0.2% of the $Z_c(3900)^\pm$ total width. As $\omega\pi$ is a typical light hadron decay mode of a $I^G(J^P) = 1^+(1^+)$ resonance, the non-observation of $Z_c(3900)^\pm \to \omega\pi^\pm$ may indicate that the

annihilation of $c\bar{c}$ in $Z_c(3900)^{\pm}$ is suppressed. Complementary to the searches for $Z_c(3900)$ production [18–20], exploring new $Z_c(3900)$ decay modes may provide a significant input to clarify its dynamical origin.

ACKNOWLEDGMENTS

The BESIII Collaboration thanks the staff of BEPCII and the IHEP computing center for their strong support. This work is supported in part by the National Key Basic Research Program of China under Contract No. 2015CB856700; the National Natural Science Foundation of China (NSFC) under Contracts No. 11125525, No. 11235011, No. 11322544, No. 11335008, No. 11425524; the Chinese Academy of Sciences (CAS) Large-Scale Scientific Facility Program; Joint Large-Scale Scientific Facility Funds of the NSFC and CAS under Contracts No. 11179007, No. U1232201, No. U1332201; CAS under Contracts No. KJCX2-YW-N29, No. KJCX2-YW-N45; the 100 Talents Program of CAS; the INPAC and Shanghai Key Laboratory for Particle Physics and Cosmology; German Research Foundation DFG under Contract No. Collaborative Research Center CRC-1044; the Istituto Nazionale di Fisica Nucleare, Italy; the Ministry of Development of Turkey under Contract No. DPT2006K-120470; the Russian Foundation for Basic Research under Contract No. 14-07-91152; the U.S. Department of Energy under Contracts No. DE-FG02-04ER41291, No. DE-FG02-05ER41374, No. DE-FG02-94ER40823, No. DESC0010118; the U.S. National Science Foundation; the University of Groningen (RuG) and the Helmholtzzentrum fuer Schwerionenforschung GmbH (GSI), Darmstadt; and the WCU Program of National Research Foundation of Korea under Contract No. R32-2008-000-10155-0.

[1] M. Ablikim *et al.* (BESIII Collaboration), Observation of a Charged Charmoniumlike Structure in $e^+e^- \to \pi^+\pi^- J/\psi$ at $\sqrt{s} = 4.26$ GeV, Phys. Rev. Lett. **110**, 252001 (2013).

[2] Z. Q. Liu *et al.* (Belle Collaboration), Study of $e^+e^- \to \pi^+\pi^- J/\psi$ and Observation of a Charged Charmoniumlike State at Belle, Phys. Rev. Lett. **110**, 252002 (2013).

[3] T. Xiao, S. Dobbs, A. Tomaradze, and K. K. Seth, Observation of the charged hadron $Z_c^{\pm}(3900)$ and evidence for the neutral $Z_c^0(3900)$ in $e^+e^- \to \pi\pi J/\psi$ at $\sqrt{s} = 4170$ MeV, Phys. Lett. B **727**, 366 (2013).

[4] M. Ablikim *et al.* (BESIII Collaboration), Observation of $Z_c(3900)^0$ in $e^+e^- \to \pi^0\pi^0 J/\psi$, arXiv:1506.06018.

[5] M. Ablikim *et al.* (BESIII Collaboration), Observation of a Charged $(D\bar{D}^*)^{\pm}$ Mass Peak in $e^+e^- \to \pi D\bar{D}^*$ at $\sqrt{s} = 4.26$ GeV, Phys. Rev. Lett. **112**, 022001 (2014).

[6] L. Maiani, V. Riquer, R. Faccini, F. Piccinini, A. Pilloni, and A. D. Polosa, A $J^{PG} = 1^{++}$ charged resonance in the $Y(4260) \to \pi^+\pi^- J/\psi$ decay?, Phys. Rev. D **87**, 111102 (2013).

[7] M. B. Voloshin, $Z_c(3900)$—what is inside?, Phys. Rev. D **87**, 091501 (2013).

[8] F.-K. Guo, C. Hidalgo-Duque, J. Nieves, and M. P. Valderrama, Consequences of heavy quark symmetries for hadronic molecules, Phys. Rev. D **88**, 054007 (2013).

[9] Q. Wang, C. Hanhart, and Q. Zhao, Decoding the Riddle of $Y(4260)$ and $Z_c(3900)$, Phys. Rev. Lett. **111**, 132003 (2013).

[10] D.-Y. Chen, X. Liu, and T. Matsuki, Predictions of Charged Charmoniumlike Structures with Hidden-Charm and Open-Strange Channels, Phys. Rev. Lett. **110**, 232001 (2013).

[11] E. S. Swanson, Coupled channel cusps and $Z_b(10610)$, $Z_b(10650)$, and $Z_c(3900)$, Phys. Rev. D **91**, 034009 (2015).

[12] S. Prelovsek and L. Leskovec, Evidence for $X(3872)$ from DD^* Scattering on the Lattice, Phys. Rev. Lett. **111**, 192001 (2013).

[13] S. Prelovsek and L. Leskovec, Search for $Z_c^+(3900)$ in the 1^{+-} channel on the lattice, Phys. Lett. B **727**, 172 (2013).

[14] S. Prelovsek, C. B. Lang, L. Leskovec, and D. Mohler, Study of the Z_c^+ channel using lattice QCD, Phys. Rev. D **91**, 014504 (2015).

[15] L. Leskovec, S. Prelovsek, C. B. Lang, and D. Mohler, Study of the Z_c^+ channel in lattice QCD, arXiv:1410.8828.

[16] S. h. Lee *et al.* (Fermilab Lattice and MILC Collaborations), Searching for the $X(3872)$ and $Z_c^+(3900)$ on HISQ lattices, arXiv:1411.1389.

[17] Y. Chen, M. Gong, Y. H. Lei, N. Li, J. Liang, C. Liu, H. Liu, J. L. Liu *et al.*, Low-energy scattering of $(D\bar{D}^*)^{\pm}$ system and the resonance-like structure $Z_c(3900)$, Phys. Rev. D **89**, 094506 (2014).

[18] R. Aaij *et al.* (LHCb Collaboration), Measurement of the resonant and CP components in $\bar{B}^0 \to J/\psi\pi^+\pi^-$ decays, Phys. Rev. D **90**, 012003 (2014).

[19] K. Chilikin *et al.* (Belle Collaboration), Observation of a new charged charmoniumlike state in $\bar{B}^0 \to J/\psi K^-\pi^+$ decays, Phys. Rev. D **90**, 112009 (2014).

[20] C. Adolph *et al.* (COMPASS Collaboration), Search for exclusive photoproduction of $Z_c^{\pm}(3900)$ at COMPASS, Phys. Lett. B **742**, 330 (2015).

[21] F. E. Close and S. Godfrey, Charmonium hybrid production in exclusive B meson decays, Phys. Lett. B **574**, 210 (2003).

[22] E. Braaten and M. Kusunoki, Low-energy universality and the new charmonium resonance at 3870 MeV, Phys. Rev. D **69**, 074005 (2004).

[23] M. Ablikim *et al.* (BESIII Collaboration), Design and construction of the BESIII detector, Nucl. Instrum. Methods Phys. Res., Sect. A **614**, 345 (2010).

[24] M. Ablikim *et al.* (BESIII Collaboration), Precision measurement of the integrated luminosity of the data taken by BESIII at center of mass energies between 3.810 GeV and 4.600 GeV, arXiv:1503.03408.

[25] S. Agostinelli *et al.* (GEANT4 Collaboration), GEANT4: A simulation toolkit, Nucl. Instrum. Methods Phys. Res., Sect. A **506**, 250 (2003).

[26] D. J. Lange, The EvtGen particle decay simulation package, Nucl. Instrum. Methods Phys. Res., Sect. A **462**, 152 (2001).

[27] R.-G. Ping, Event generators at BESIII, Chin. Phys. C **32**, 599 (2008).

[28] S. Jadach, B. F. L. Ward, and Z. Was, The precision Monte Carlo event generator KK for two fermion final states in e^+e^- collisions, Comput. Phys. Commun. **130**, 260 (2000).

[29] S. Jadach, B. F. L. Ward, and Z. Was, Coherent exclusive exponentiation for precision Monte Carlo calculations, Phys. Rev. D **63**, 113009 (2001).

[30] K. A. Olive *et al.* (Particle Data Group Collaboration), Review of particle physics, Chin. Phys. C **38**, 090001 (2014).

[31] J. C. Chen, G. S. Huang, X. R. Qi, D. H. Zhang, and Y. S. Zhu, Event generator for J/ψ and $\psi(2S)$ decay, Phys. Rev. D **62**, 034003 (2000).

[32] T. Sjostrand, S. Mrenna, and P. Z. Skands, PYTHIA 6.4 physics and manual, J. High Energy Phys. 05 (2006) 026.

[33] H. Albrecht *et al.* (ARGUS Collaboration), Search for hadronic $b \to u$ decays, Phys. Lett. B **241**, 278 (1990).

[34] S. Actis *et al.* (Working Group on Radiative Corrections and Monte Carlo Generators for Low Energies Collaboration), Quest for precision in hadronic cross sections at low energy: Monte Carlo tools vs. experimental data, Eur. Phys. J. C **66**, 585 (2010).

[35] M. Ablikim *et al.* (BESIII Collaboration), Branching fraction measurements of χ_{c0} and χ_{c2} to $\pi^0\pi^0$ and $\eta\eta$, Phys. Rev. D **81**, 052005 (2010).

[36] M. Ablikim *et al.* (BESIII Collaboration), Study of $a_0^0(980) - f_0(980)$ mixing, Phys. Rev. D **83**, 032003 (2011).

[37] M. Ablikim *et al.* (BESIII Collaboration), Search for hadronic transition $\chi_{cJ} \to \eta_c\pi^+\pi^-$ and observation of $\chi_{cJ} \to K\bar{K}\pi\pi\pi$, Phys. Rev. D **87**, 012002 (2013).